International Journal of Pure and Applied Mathematics
Volume 117 No. 15 2017, 599-619
ISSN: 1311-8080 (printed version); ISSN: 1314-3395 (on-line version)
url: http://www.ijpam.eu
Special Issue

ijpam.eu

A Novel approach for Multimodal Medical Image Fusion using Hybrid Fusion Algorithms for Disease Analysis

B.Rajalingam[1], Dr.R.Priya[2]
[1]Research Scholar, [2]Associate Professor
Department of Computer Science & Engineering, Annamalai University,
Chidambaram, Tamilnadu, India
rajalingam35@gmail.com[1], prykndn@yahoo.com[2]

Abstract

Multimodality medical image fusion technique performs a vital role in biomedical research and clinical disease analysis. The medical image fusion is used to improve the quality of multimodality medical images by merge the two multimodal medical images of the same patient. This paper, proposed a novel multimodal medicinal image fusion approach based on hybrid fusion techniques. Magnetic Resonance Imaging (MRI), Positron Emission Tomography (PET) and Single Photon Emission Computed Tomography (SPECT) are the input multimodal therapeutic brain images and the curvelet transform with neural network techniques are applied to fuse the multimodal medical image. Along with, Subband Decomposition, Dividing the multimodal medical image into resolution layers, Smooth Partitioning used smoothly squares input medical images with appropriate scale. Ridgelet Transform techniques was used along with radon Transform to execute multimodal medical image to convert from 1-D to 2-D image in the restoration level, after reconstructed multimodality medical image applied the pulse coupled neural network fusion rule to get the fused medical image. The proposed work combines the curvelet transform with pulse coupled neural network for fusion process. Hybrid fusion algorithms are evaluated using several performance quality metrics. Compared with other existing techniques the proposed technique experimental results demonstrate the better processing performance and results in both subjective and objective evaluation criteria.

Keywords: Multimodal medical image fusion, MRI, PET, SPECT, PCA, DWT, DCHWT, GIF, curvelet transform, Sub-band Decomposition, Ridgelet Transform and PCNN.

1 Introduction

Image fusion is the mixture of two or more different images to form a novel image by using certain techniques. It is extracting information from multi-source images and improves the spatial resolution for the original multi-spectral image and preserves the spectral information. Image fusion can be done in three levels: Pixel level fusion, Feature level fusion and Decision level fusion. Pixel-level fusion having a large portion of the remarkable data is protected in the merged image. Feature-level fusion performs on feature-by-feature origin, such as edges, textures. Decision-level fusion refers to make a final merged conclusion. The image fusion decrease quantity of information and hold vital data. It make new output image that is more appropriate for the reasons for human/machine recognition or for further processing tasks. Image fusion is classified into two types' single sensor and multi sensor picture combination consolidating the pictures from a few sensors to shape a composite

picture and their individual pictures are converged to acquire an intertwined image Ex: Multi focus and Multi Exposure fusion.

Multi sensor image fusions merge the images from several sensors to form a composite image and their individual images are merged to obtain a fused image. Ex: medical imaging, military area. Multimodality medical images categorised into several types which include computed tomography (CT), magnetic resonance angiography (MRA), magnetic resonance imaging (MRI), positron emission tomography (PET), ultra sonography (USG), nuclear magnetic resonance(NMR) spectroscopy, single photon emission computed tomography (SPECT), X-rays, visible, infrared and ultraviolet. MRI, CT, USG and MRA images are the structural therapeutic images which afford lofty resolution images. PET, SPECT and functional MRI (fMRI) images are functional therapeutic images which afford low-spatial resolution images with functional information. Anatomical and functional therapeutic images can be incorporated to obtain more constructive information about the same object. Medicinal image fusion reduces storage cost by storing the single fused image instead of multiple-input images. Multimodal medical image fusion uses the pixel level fusion. Different imaging modalities can only provide limited information. Computed Tomography (CT) image can display accurate bone structures. Magnetic Resonance Imaging (MRI) image can reveal normal and pathological soft tissues. The fusion of CT and MRI images can integrate complementary information to minimize redundancy and improve diagnostic accuracy. Combined PET/MRI imaging can extract both functional information and structural information for clinical diagnosis and treatment. Image fusion having several applications like medical imaging, biometrics, automatic change detection, machine vision, navigation aid, military applications, remote sensing, digital imaging, aerial and satellite imaging, robot vision, multi focus imaging, microscopic imaging, digital photography and concealed weapon detection. Multimodal medical imaging plays a vital role in a large number of healthcare applications including medical diagnosis and treatment. Medical image fusion combining multiple images into form a single fused modalities. Medical image fusion methods involve the fields of image processing, computer vision, pattern recognition, machine learning and artificial intelligence.

The research paper is organized as follows. Sec. 2 describes the literature survey on related works. Sec. 3 discusses the proposed research work method both traditional and hybrid multimodal medical image fusion techniques, performance evaluation metrics is briefly reviewed. Sec. 4 describes the implemented medical image fusion experimental results and performance comparative analysis. Finally, Sec. 5 concludes the paper.

2 Related Works

Jiao Du, Weisheng Li, Ke Lu.[1] proposed the multimodal medicinal image fusion for the image disintegration, image restoration, image mixture rules and image excellence assessments. Therapeutic image fusion has been broadly used in medical assessments for disease diagnose. Xiaojun Xua, Youren Wang, et al. [2] proposed a multimodality medicinal image mixture algorithm based on discrete fractional wavelet transform. The input therapeutic images are decomposed using discrete fractional wavelet transform. The sparsity character of the mode coefficients in subband images changes. Xingbin Liu, Wenbo Mei, et al.[3] proposed a new technique namely Structure tensor and non subsampled shearlet transform (NSST) to extract geometric features. A novel unified optimization model is proposed for

fusing computed Tomography (CT) and Magnetic Resonance Imaging (MRI) images. K.N. Narasimha Murthy and J. Kusuma[4] proposed Shearlet Transform (ST) to fuse two different images Positron Emission Tomography (PET) and Magnetic Resonance Imaging (MRI) image by using the Singular Value Decomposition (SVD) to improve the information content of the images. Satishkumar S. Chavan, Abhishek Mahajan,et al.[5] introduced the technique called Nonsubsampled Rotated Complex Wavelet Transform (NSRCxWT) combining CT and MRI images of the same patient. It is used for the diagnostic purpose and post treatment review of neurocysticercosis. S. Chavan, A. Pawar, et al.[6] innovated a feature based fusion technique Rotated Wavelet Transform (RWT) and it is used for extraction of edge-related features from both the source modalities (CT/MRI). Heba M. El-Hoseny, El-Sayed M.El.Rabaie,et al.[7] proposed a hybrid technique that enhance the fused image quality using both traditional and hybrid fusion algorithms(Additive Wavelet Transform (AWT) and Dual Tree complex wavelet transform (DT-CWT)). Udhaya Suriya TS, Rangarajan P [8] implemented an innovative image fusion system for the detection of brain tumours by fusing MRI and PET images using Discrete Wavelet Transform (DWT). Jingming Yang, YanyanWu,et al.[9] described an Image fusion technique Non-Subsampled Contourlet Transform (NSCT) to decompose the images into lowpass and highpass subbands. C.Karthikeyan, B. Ramadoss[10] proposed the fusion of medical images using dual tree complex wavelet transform (DTCWT) and self organizing feature map (SOFM) for better disease diagnosis. Xinzheng Xu,Dong Shana,et al.[11] introduced an adaptive pulse-coupled neural networks (PCNN), which was optimized by the quantum-behaved particle swarm optimization (QPSO) algorithm to improve the efficiency and quality of QPSO. Three performance evaluation metrics is used. Jyoti Agarwaland Sarabjeet Singh Bedi, et al.[12] innovate the hybrid technique using curvelet and wavelet transform for the medical diagnosis by combining the Computed Tomography (CT) image and Magnetic Resonance Imaging (MRI) image. Jing-jing Zonga and Tian-shuang Qiua[13] proposed a new fusion scheme for medical images based on sparse representation of classified image patches In this method, first, the registered input images are separated into confidential patches according to the patch geometrical route, from which the corresponding sub-dictionary is trained via the online dictionary learning (ODL) algorithm and the least angle regression (LARS) algorithm to sparsely code each patch; second, the sparse coefficients are combined with the "choose-max" fusion rule; Finally, the fused image is reconstructed from the combined sparse coefficients and the corresponding sub-dictionary. Richa Gautam and Shilpa Datar[14] proposed a method for fusing CT (Computed Tomography) and MRI (Medical Resonance Imaging) images based on second generation curvelet transform. Proposed method is compared with the results obtained after applying the other methods based on Discrete Wavelet Transform (DWT), Principal Component Analysis (PCA) and Discrete Cosine Transform (DCT). Jiao Du, Weisheng Li, Bin Xiao,et.al.[15] proposed an approach union Laplacian pyramid with multiple features for accurately transferring salient features from the input medical images into a single fused image. Zhaobin Wang, Shuai Wang,Ying Zhu,et al.[16] described the statistical analysis PCNN and some modified models are introduced and reviewed the PCNN's applications in the field of image

fusion. Zhaobin Wang, Shuai Wang, et al.[17] Proposed a novel guided filtering based weighted average technique to make full use of spatial consistency for fusion of the base and detail layers. B. K. Shreyamsha Kumar [18] proposed a discrete cosine harmonic wavelet transform (DCHWT) based image fusion to retain the visual quality and performance of the merged image with reduced computations.

3 Proposed Research Work

3.1 Traditional Multimodal Medical Image Fusion Techniques

This paper implements different traditional image fusion algorithms for different types of multimodality medical images as shown in Figure. 1

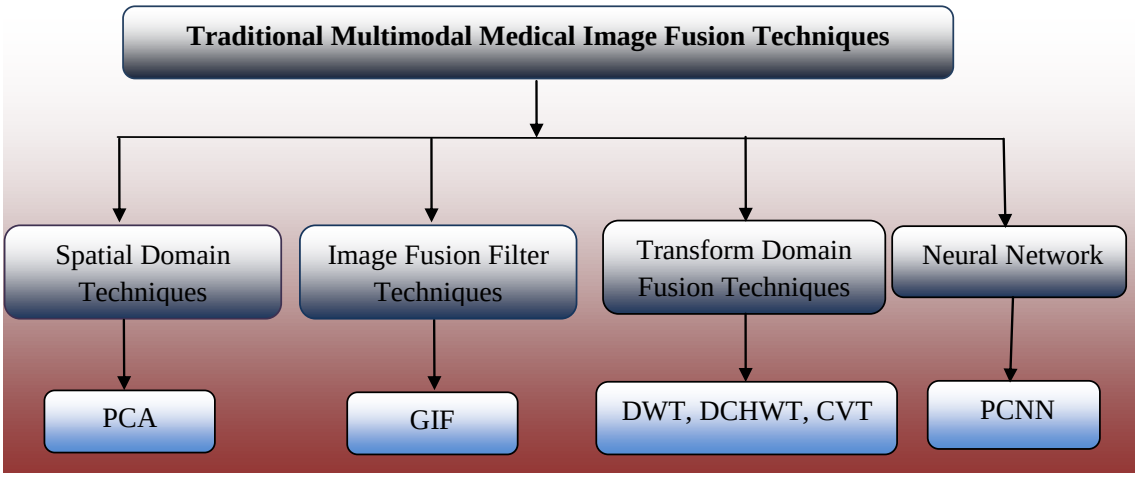

Figure 1 Traditional multimodal medical image fusion techniques

3.1.1 Principal Component Analysis (PCA)

Principal Component Analysis (PCA) is one of the well-known techniques used for measurement decrease, feature removal and data revelation. In general, PCA is defined by the conversion of an elevated dimensional vector space into a near to the ground dimensional vector space. This property of principal component analysis is helpful in reducing the size of medical image data which is of large size without losing essential information. In this method a number of simultaneous variables are altered into uncorrelated variables called principal components. Each principal component is taken in the route of highest variance and lie in the subspace at right angles to one another.

3.1.1.1 Procedural steps for image fusion using PCA algorithm

1) Convert the two input multimodal images into column vectors and make a matrix ‘B’ using these two column vectors.
2) Calculate the empirical mean vector along each column and subtract it from each of the columns of the matrix.
3) Calculate the covariance matrix ‘R’ of the resulting matrix.
4) Calculate the eigen values K and eigen vectors E of the covariance matrix.
5) Select the eigenvector equivalent to well-built eigen value and divide its each element by mean of that eigenvector. This will give us first principal component P1. Repeat the same procedure with eigenvector corresponding to smaller eigen value to get second principal component P2.

$$P_1 = \frac{R(1)}{\sum R} \quad P_2 = \frac{R(2)}{\sum R}$$

6) Final Fused multimodal medical image is obtained by

$$I_f(x,y) = P_1 I_1(x,y) + P_2 I_2(x,y) \tag{1}$$

3.1.2 Image Fusion with Guided Filtering

Currently, in medical image processing energetic research topic is edge preserving filter technique. Image processing has several edge preserving smoothing filtering techniques such as guided filter, weighted least squares and bilateral filter. Among the several filter techniques the guided image filter is giving better results and less execution time for fusion process. This image fusion filter method is based on a local linear form, creating it eligible for other image processing methods such as image matting, up-sampling and colorization. A multi-level representation is utilized by average smoothing filter. Subsequently, based on weighted average fusion technique, the guided image filter fuses the bottom and feature layers of multi-modal medical images.

3.1.2.1 Multi level Image Decomposition

The average filter used to decompose the input multimodal medical images into multilevel representations. The bottom layer of each input image is represented by.

$$\boldsymbol{E}_n = S_n * K \tag{2}$$

Where the n^{th} input image is denoted as S_n, average filter is represented by K and the 31×31 conventional matrix is set to average filter size. First the bottom layer is found then the feature layer can be simply computed by subtracting the bottom layer from the input medical images.

$$\boldsymbol{F}_n = S_n - E_n \tag{3}$$

The aim of the multi level decomposition step is to separate each input medical images into bottom and feature layer. A bottom layer contains the huge level variations in strength and a feature layer contains the minute level information.

3.1.2.2 Guided image filter with weight map construction

The Gaussian filtering is applied on both the input multimodality medical images to get the high pass multimodal medical image R_n.

$$\boldsymbol{R}_n = S_n * M \tag{4}$$

Where the Gaussian filters is represented by M with 3 × 3 matrix. Construct the saliency maps P_n using the local average value of R_n.

$$P_n = |R_n| * v_{r_v \sigma_v} \tag{5}$$

Where Gaussian low pass filter is denoted by v and $(2r_v + 1)$ $(2r_v + 1)$ is the size of low pass filter and the r_v and σ_v parameters of the Gaussian filters. The calculated saliency weight maps are giving good description and detail information of the saliency intensity. After that, the saliency weight maps are compared to establish the weight maps are represented by,

$$T_x^k = \begin{cases} 1 \; if \; P_1^k = \max(P_1^k, P_2^k \ldots\ldots, P_X^k) \\ 0 \qquad\qquad otherwie \end{cases} \tag{6}$$

Where the number of input multimodal medical images is represented by X, the saliency value of the pixel k in the n^{th} image is P_x^k. But, the artifacts of the merged image which may produce the weight maps with noisy and not associated with object limitations. The effective way to solve the above problem is to use spatial consistency. Spatial consistency is two adjacent pixels have identical clarity or color, they will be apt to have comparable weights. The formulating an energy function is based on spatial consistency fusion approach. To get the essential weight maps this energy function can be minimized globally. But, the optimization based methods are often somewhat incompetent. Guided image filtering is

performed on every weight map T_n with the equivalent input image S_n serving as the supervision image.

$$W_n^E = V_{r_1\varepsilon_1}(T_n, S_n) \quad (7)$$

$$W_n^F = V_{r_1\varepsilon_1}(T_n, S_n) \quad (8)$$

Where the guided image filtering parameters are represented by $r_1, \varepsilon_1, r_2, and\ \varepsilon_2$, the weight maps of the bottom and features layers denoted by W_n^E and W_n^F. N is normalized weight maps value and each pixel k is sum to one. The inspiration of the weight maps construction technique is represented in the following expression. The eqn.1, eqn. 3 and eqn. 4 derived the local variance point i is referred by its value very small and the supervision image having pixel in very large, then a_k will become close to 0 and the filtering output R will equal to $\overline{T_k}$. If the local variance of pixel i having very large value, then the *i* is represent the pixel edge area, next a_k will become far from zero. As established in, $\nabla R \approx \bar{a}\,\nabla S$ will turn into accurate, which means that only the weight map in one side of the edge will be averaged. In both situations, those pixels with identical color or clarity tend to have comparable weights. In contrast, sharp and edge-aligned weights are preferred for merging the feature layers because details may be lost when the weights are over-smoothed. Hence, a large filter size and a large blur degree are chosen for merging the bottom layers, while a minute filter size and a minute blur degree are chosen for the feature layers.

3.1.2.3 Multi level Image re-enactment

Multi level image reconstruction contains the following two steps. Initially, the bottom and feature layers of different input multimodal medical images are combined together using weighted averaging filtering

$$\bar{E} = \sum_{n=1}^{N} W_n^E \boldsymbol{E}_n \quad (9)$$

$$\bar{F} = \sum_{n=1}^{N} W_n^F \boldsymbol{F}_n \quad (10)$$

Next, the merged output multimodal medical image R is obtained by combining the merged bottom layer $\bar{E}$ and the merged feature layer $\bar{F}$

$$R = \bar{E} + \bar{F} \quad (11)$$

3.1.2.4 Procedural steps for image fusion using Guided Image Filtering:

1) Take the two input multimodal medical images.
2) Resize both images into 512 x 512 dimensions.
3) Decompose the input multimodal medical images using average filtering.
4) Separate the input multimodality medical images into bottom layer and feature layer based on multi scale representation.
5) Apply the Gaussian laplacian filters for to construct the weight map and saliency map.
6) Perform the image reconstruction and get the final fused multimodal medical image.

3.1.3 Discrete Wavelet Transform (DWT)

Wavelet transform is applied in two domains namely continuous and discrete. CWT (Continuous Wavelet Transform) is the correlation between the wavelet at different scales (inverse of frequency) and the signal and is figured by changing the size of the investigation window each time, moving it, increasing it by the flag. Scientific condition is given by

$$\varphi_x(\tau, R) = \frac{1}{\sqrt{R}} \int X(t).\varphi * \left(t - \frac{\tau}{R}\right) dt \quad (12)$$

In the above expression τ (translation) and R (scale) are variables required for transforming the signal x (t). Psi (Ψ) is the transforming function known as mother wavelet. In DWT (Discrete Wavelet Transform) a 2D signal (image) I(x, y) is first filtered through low pass and high pass finite impulse response filters (FIR), having impulse response h[n] in horizontal direction and then decimated by factor of 2. This gives first level decomposition. Further the low pass filtered image is again filtered through low pass and high pass FIR filters in vertical

direction and then again decimated by 2 to obtain second level decomposition. Filtering operation is given by the convolution of the signal and impulse response of signal.

$$X[n] * h[n] = \sum_{k=-\infty}^{\infty} X[k].h[n-k] \quad (13)$$

Now to perform inverse wavelet transform, first up sample the sub band images by factor of 2 column wise and then filter them through low pass and high pass FIR filters. Repeat the same process in next step row wise. Now add all the images to get the original image.

3.1.3.1 Procedural steps for image fusion using DWT algorithm

1) Take the two input multimodal medical images.
2) Resize both images into 512 x 512 dimensions.
3) Convert both the images into gray scale if required.
4) Apply 2D-DWT on both the images and obtain its four components.
5) Now apply the fusion rule as per the requirement.

a) Most extreme pixel determination governs (all maximum): By choosing every single greatest coefficient of both the input images and merging them.
b) Mean: By taking the normal of the coefficients of both the images.
c) Blend: By taking the normal of the estimated coefficients of both the input images and choosing the most extreme pixels from detail coefficients of both the input data.

6) Now apply IDWT to obtain the fused output image.

3.1.4 Discrete cosine harmonic wavelet transforms (DCHWT)

A DCT expresses a predetermined order of data indicated in terms of a sum of cosine functions alternate at different frequencies. The discrete cosine transform generate the signal in the symmetric cyclic order and remove the discontinuity symmetric signal to move from one step to next step efficiently. The extension of the symmetric signal make the length into double for the original signal and giving better frequency resolution for factor of two.

$A_E(t)$ and $\psi_E(t)$ are denoted as real symmetric signal and real symmetric wavelet function respectively.

$$R_c(x,y) = \frac{|x|^{\frac{1}{2}}}{2\pi} \int_{-\infty}^{\infty} A_E(\sigma)\, \Psi_E(x\sigma) \cos(\sigma y)\, d\sigma \quad (14)$$

Where the cosine transforms are represented by $A_E(\sigma)$ and $e(\sigma)$ of wavelet functions $A_E(t)$ and $\psi_E(t)$, respectively. The wavelet transform $R_c(x,y)$ used in the cosine domain moderately than the Fourier domain. Consequently, Eq. 13 can be modified as

$$R_c(x,y) = |x|^{\frac{1}{2}} \quad ^{-1}[R_E(\sigma)\Psi_E(x\sigma)] \quad (15)$$

In Eq.14 cosine transform functions $A_E(\sigma)$ and $e(\sigma)$ are used to compute the cosine wavelet coefficients $R_c(x,y)$ for a particular scale *x*. The harmonic wavelet function is denoted as $\Psi(\sigma)$ in harmonic wavelet transform, the cosine harmonic wavelet function $s(\sigma)$ is easy and it is zero for all frequencies apart from the small frequency band where it is stable, It is referred by.

$$\Psi_E(\sigma) = \begin{cases} 1, \sigma_c - \sigma_0 < \sigma < \sigma_c + \sigma_0, \\ -\sigma_c - \sigma_0 < \sigma - \sigma_c + \sigma_0, \\ 0, \quad \text{elsewhere} \end{cases} \quad (16)$$

The equivalent wavelet $\varphi_E(t)$ in time domain is converted into.

$$\Psi(t) = \frac{\sigma_0}{\pi} \frac{\sin \sigma_0 t}{\sigma_0 t} \cos(\sigma_c t)$$
$$= \frac{\sigma_0}{\pi} \sin c(\sigma_0 t) \cos(\sigma_c t) \quad (17)$$

The Shannon scaling function is a cosine modulated edition of the protect wavelet. The symmetric rectangular function and for a discrete signal, it is zero apart from on symmetric

finite bands [π/c, π/d] and [−π/c, −π/d] where c, d can be real numbers for the spectral weighing in cosine harmonic transform. The cosine harmonic transform too suffers from the difficulty of poor time localization and the result of spectral weighing to restrict in time period by wavelet functions other than rectangular outputs in non orthogonal wavelets due to spectral overlap similar to the Fourier based harmonic wavelet transform. In discrete cosine harmonic wavelet transform the multimodal medical image is decomposed by cluster the discrete cosine transform coefficients in a method similar to that of discrete Fourier transform coefficients except for the conjugate procedure in inserting the coefficients symmetrically. The inverse discrete cosines transform of these collection results in discrete cosine harmonic wavelet coefficients. The discrete cosine transform of these progression subbands results in subband DCT coefficients, which are relocated in their equivalent spot to recover the overall DCT range at the unique sampling rate.

3.1.4.1 Procedural steps for image fusion using DCHWT algorithm

1) Take the two source multimodal medical images.
2) Resize both images into 512 x 512 dimensions
3) Divide the first 2D image into rows and link them together in a chain form to have a 1D row vector R.
4) Divide the second 2D image into columns and link them together in a chain form to have a 1D column vector C.
5) Apply DCHWT on both R and C separately and then apply averaging operation on the vectors.
6) Apply inverse DCHWT on the resulting vector.
7) Convert 1D vector into 2D image to obtain the fused output medical image

3.1.5 Curvelet Transform Techniques

Curvelet transform method is based on medical image segmentation which divides the input multimodal medical image into number of small overlapping tiles and ridegelet transform is applied to each of the tiles to perform edge detection. The resulting fused output multimodality medical image provides more information by preventing image denoising. Curvelet transform results giving superior performance than other transform techniques in terms of signal to noise ratio value. The curvelet transform method classified into four stages such as Subband Decomposition, Smooth Partitioning, Renormalization and Ridgelet analysis.

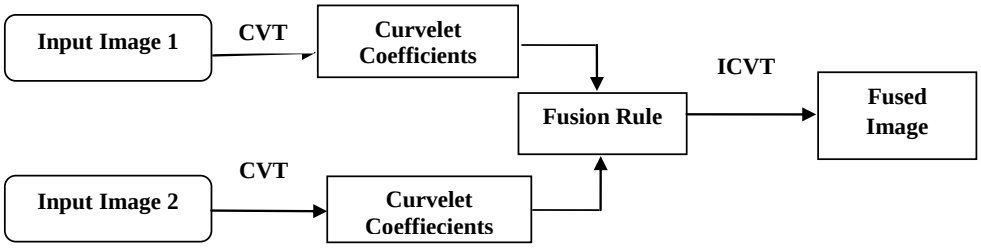

Figure.2 Image Fusion Process of Curvelet Transform

3.1.5.1. Sub-band decomposition

The input multimodal medical image is first decomposed into wavelet sub-bands and then Curvelet subbands are formed by performing partial image reconstruction from these wavelet sub-bands at various levels.

$$f \mapsto (P_0 f, \Delta_1 f, \Delta_2 f, \ldots) \tag{18}$$

Divide the multimodal medical image into resolution layers. Each layer contains details of different frequencies: P0 – Low-pass filter. Δ_1, Δ_2 – Band-pass (high-pass) filters.

The original image can be reconstructed from the sub-bands:

$$f = P_0(P_0 f) + \sum_s \Delta_s(\Delta_s f) \tag{19}$$

Energy preservation

$$\|f\|_2^2 = \|P_0 f\|_2^2 + \sum_s \|\Delta_s f\|_2^2 \tag{20}$$

3.1.5.2. Smooth partitioning

The decomposed multimodal medical image each subband is smoothly windowed in to 'squares' of an appropriate scale.

$$h_Q = w_Q \cdot \Delta_s f \tag{21}$$

3.1.5.3. Renormalization

The outcome of the smoothening multimodal medical image of each resulting square is renormalized to unit scale.

$$g_Q = T_Q^{-1} h_Q \tag{22}$$

3.1.5.4. Ridgelet analysis

In the earlier two levels we transform the multimodal medical image curved lines into small straight lines. That improves the ability of the Curvelet transform to handle the medical image curved edges.

Ridgelet Transform: The Ridgelet Transform deals efficiently with line singularities in 2D. The basic idea is to map a line singularity in the two-dimensional (2D) domain into a point by means of the Radon transform. Then, a one-dimensional wavelet is performed to deal with the point singularity in the Radon domain

$$\alpha_{(Q,\lambda)} = \langle g_Q, \rho_\lambda \rangle \tag{23}$$

3.1.5.5 Procedural steps for image fusion using Curvelet Transform algorithm

1) Take the two input multimodal medical images.
2) Resize both images into 512 x 512 dimensions.
3) Each input multimodal medical image is then analyzed and a set of Curvelet coefficients are generated
4) Maximum Selection, Minimum Selection and Simple Average fusion rules are applied.
5) Finally apply the Inverse Curvelet transform (ICVT) to reconstruct the multimodal source image.
6) Perform the image reconstruction and get the final fused multimodal medical image.

3.1.6 PCNN Model

Pulse coupled neural network system (PCNN) is a novel visual cortex roused neural system portrayed by the worldwide coupling and heartbeat synchronization of neurons. The basic PCNN model demonstrated in the Figure.3, which incorporates three sections: open field, modulation field and heartbeat generator. The equation for streamlined PCNN can be communicated as

$$E_{ij}(r) = T_{ij} \tag{24}$$

$$S_{ij}(r) = e^{-a^L} S_{ij}(r-1) + X^L \textstyle\sum_{kj} Y_{kj} R_{ijkl}(r-1) \tag{25}$$

$$V_{ij}(r) = E_{ij}(r)[1 + \beta S_{ij}(r)] \tag{26}$$

$$\theta_{ij}(r) = e^{-a^\theta} \theta_{ij}(r-1) + X_{ij}^\theta R_{ij}(r-1) \tag{27}$$

$$R_{ij}(r) = step\left(V_{ij}(r) - R_{ij}(r)\right) = \begin{cases} 1, & U_{ij}(r) > \theta_{ij}(r) \\ 0, & otherwise \end{cases} \tag{28}$$

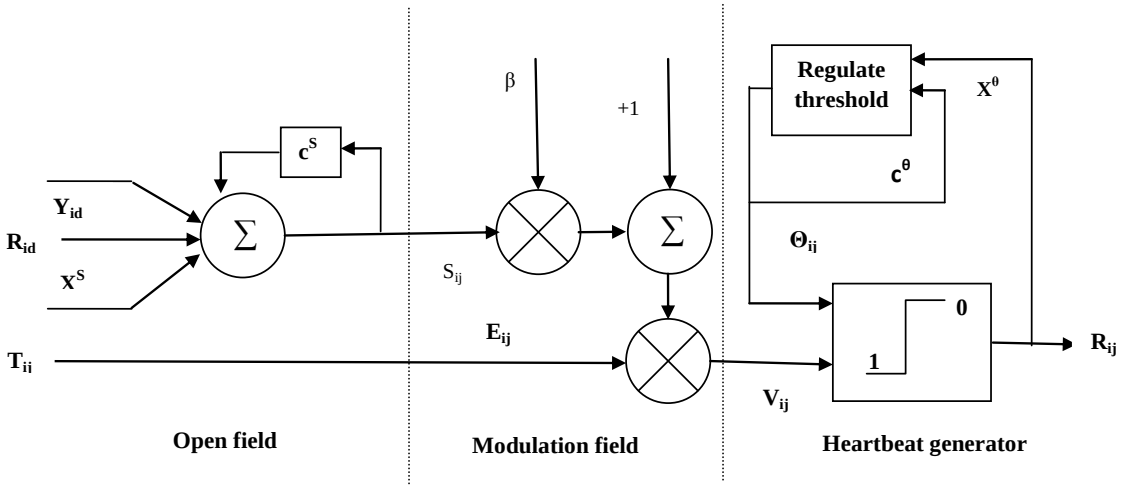

Figure 3 Simplified PCNN model

In Fig. 2, the open field contains two input compartment: the feeding E_{ij} and the connecting S_{ij} (see (17) and (18)). Each neuron receives the output R_{ij} of neighborhood neurons and the peripheral stimuli T_{ij}, where T_{ij} represent the gray value of the input image. In the modulation field, the domestic state signal V_{ij} is created by connecting input signal S_{ij} and the feeding input E_{ij} via connecting coefficient β. Then, if V_{ij} is superior to the threshold value θ_{ij} of the neuron, the heartbeat generator will produce a pulse, namely, it is called a fire. After the neuron outputs a pulse, the threshold of the neuron will get higher rapidly by feedback. If θ_{ij} is superior to V_{ij}, the heartbeat generator stops generating the pulse, the threshold starts to reduce until θ_{ij} is less than V_{ij} again. Y_{id} denotes the connecting weight, the decay coefficients c^{S}, c^{θ} and potentials coefficients X^{S}, X^{θ} undertaking the periodicity of the pulse output of the PCNN model.

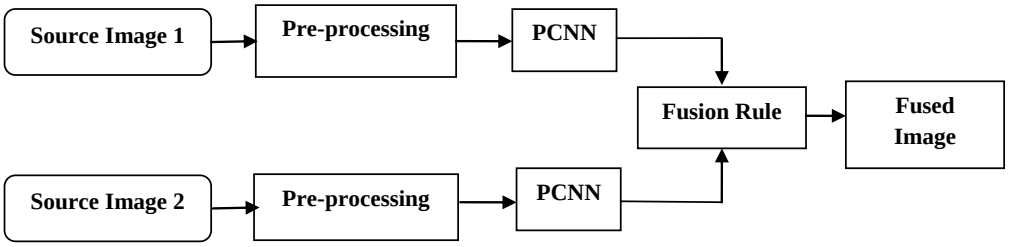

Figure.4 Image Fusion Process of PCNN

3.2 Hybrid Multimodal Medical Image Fusion Techniques

Traditional medical image fusion techniques lack the ability to get high-quality images. So, there is a bad need to use hybrid fusion techniques to achieve this objective. The basic idea of the hybrid technique is to combine the guided image filter fusion technique with neural network fusion techniques to improve the performance and increase fused image quality. Another possibility is applying two stage transformations on input images before fusion process. These transformations provide better characterization of input images, better handling of curved shapes and higher quality for fused details. The overall advantages of the hybrid techniques are improving the visual quality of the images, and decreasing image artifacts and noise. Each image size is 512*512 dimensions. Figure 4 illustrates the schematic diagram of the proposed hybrid multimodal medical image fusion techniques.

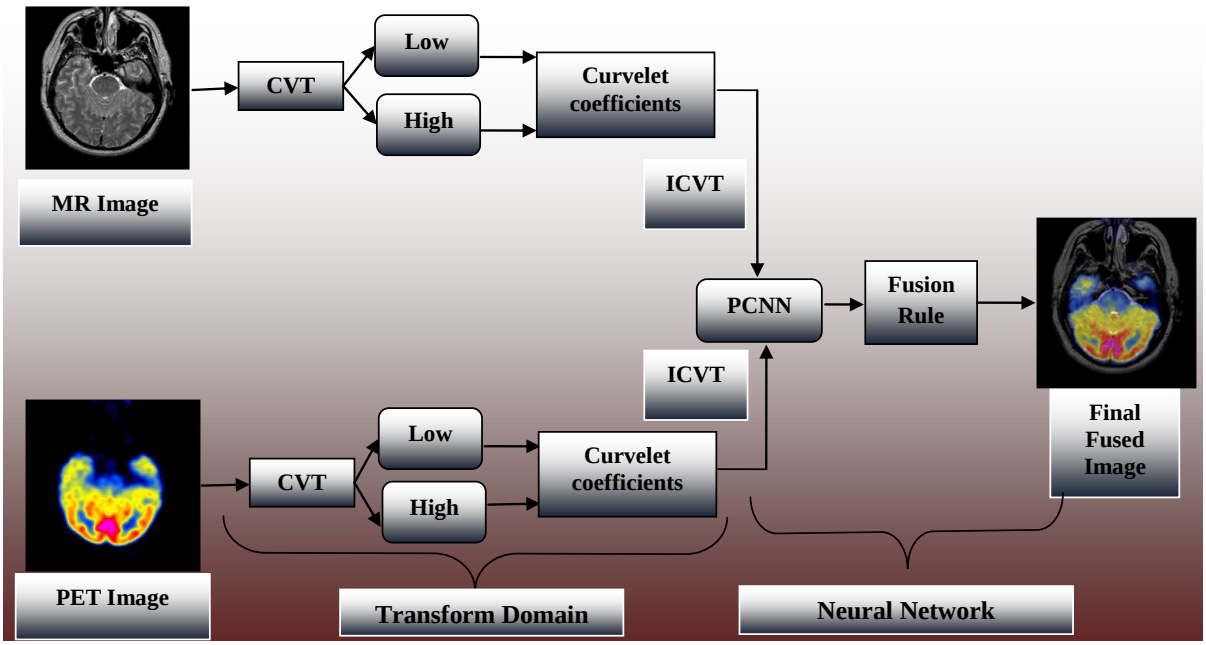

Figure.5 Overall Structure of the proposed hybrid multimodal medical image fusion algorithms

3.2.1 Proposed hybrid multimodal image fusion algorithm (CVT-PCNN)

In this proposed research work applied both Curvelet Transform and PCNN techniques on the input source multimodal medical images.

Input: CT/MRI and PET/SPECT are the two inputs of multimodal medical images which need to be processed.
Output: Multimodality medical image which is getting fused.

Step 1: The input source multimodal medical images are registered and analyzed then set of Curvelet coefficients are generated.
Step 2: Maximum Selection, Minimum Selection and Simple Average fusion rules are applied.
Step 3: Perform the reconstruction operation on the both bottom layer and feature layers of different input images.
Step 4: Now apply the Inverse Curvelet transform (ICVT) to reconstruct the multimodal source image.
Step 6: Apply the pulse coupled neural network fusion rule for the accurate medical image fusion.
Step 7: Fused final output multimodal medical image is displayed.

3.3 Evaluation Metrics

Fusion quality metrics are utilized in this work to evaluate the efficiency of the fusion algorithms. These metrics are:

3.3.1 Average Gradient (g)

The average gradient represents the amount of texture variation in the image. It is calculated as:

$$g = \frac{1}{(\mathrm{R}-1)(\mathrm{S}-1)} \sum_{\mathrm{i}=1}^{(\mathrm{R}-1)(\mathrm{S}-1)} \frac{\sqrt{(\frac{\partial \mathrm{f}}{\partial \mathrm{x}})^2 + (\frac{\partial \mathrm{f}}{\partial \mathrm{x}})^2}}{2} \quad (29)$$

Where, R and S are the image dimensions of images x and y respectively.

3.3.2 Standard Deviation (STD)

It is used to establish how much difference of the data is from the average or mean value. The input data is said to be clearer if its STD value is bigger. STD is deliberate using the equation:

$$STD = \frac{\sqrt{\sum_{\mathrm{i}=1}^{\mathrm{R}} \sum_{\mathrm{j}=1}^{\mathrm{S}} |f(i,j)-\mu|^2}}{\mathrm{RS}} \quad (30)$$

Where *R* and *S* represent the dimensions of the image f(i,j), and the mean value is represented by μ .

3.3.3 Local Contrast (C_{local})

It is an index for the image quality and purity of view. It is calculated using the equation:

$$C_{local} = \frac{|\mu_{target} - \mu_{background}|}{\mu_{target} + \mu_{background}} \quad (31)$$

Where μ_{target} is the mean gray-level of the target image in the local region of interest and $\mu_{background}$ is the mean of the background in the same region. The larger value of C indicates more purity of the image.

3.3.4 Structural Similarity Index Metric (SSIM)

It is a measure of the similarity between two regions w_x and w_y of two images *x* and *y*.

$$SSIM(x,y|w) = \frac{(2\bar{w}_x\,\bar{w}_y + C_1)(2\sigma w_x w_y + c_2)}{(\bar{w}_x{}^2 + \bar{w}_y{}^2 + C_1)(\sigma^2 w_x + \sigma^2 w_y + c_2)} \quad (32)$$

Where, C_1 *and* C_2 *are* small constants. $\bar{w}_x$, $\bar{w}_y$ are the mean values of w_x and w_y. $\sigma^2 w_x$, $\sigma^2 w_y$ are the variance of w_x and w_y. $\sigma w_x w_y$ is the covariance between the two regions

3.3.5 Xydeas and Petrovic Metric ($Q^{AB/F}$)

This metric is used to measure the transferred edge information amount from source images to the fused one. A normalized weighted performance form of that metric can be calculated as following

$$Q^{AB/F} = \frac{\sum_{m=1}^{M} \sum_{n=1}^{N} (Q_{(m,n)}^{AF} W_{(m,n)}^{AF} + Q_{(m,n)}^{BF} W_{(m,n)}^{BF})}{\sum_{m=1}^{M} \sum_{n=1}^{N} W_{(m,n)}^{AF} + W_{(m,n)}^{BF}} \quad (33)$$

Where, $Q_{(m,n)}^{AF}, Q_{(m,n)}^{BF}$ is the edge information preservation value and $W_{(m,n)}^{AF}, W_{(m,n)}^{BF}$ are their weights

3.3.6 Mutual Information (MI)

MI is an index that calculates the quantity of dependency between two images (*R*, *S*), and it gives the joint distribution detachment between them using the subsequent equation:

$$I(r,s) = \sum_{y \epsilon R} \sum_{r \epsilon R} p(r,s) \log(\frac{p(r,s)}{p(r)p(s)}) \quad (34)$$

Where *p*(r) and *p*(s) are the marginal probability distribution functions of the both images, and *p*(r,s) is the joint probability distribution function.

$$MI(r,s,f) = \frac{I(r,s)+I(r,f)}{H(r)+H(s)} \quad (35)$$

Where, *H(r), H(s)* are the entropies of images r and s.

3.3.7 Feature Similarity Index Metric (FSIM)

It represents edge similarity between input images and the fused image, and it can be calculated from the following equation:

$$FSIM = \frac{\sum_{x\in\Omega} S_L(x).PC_m(x)}{\sum_{x\in\Omega} PC_m(x)} \quad (36)$$

Where, Ω is the image spatial domain, S_L (x) is the total similarity between the two images, and PC_m(x) is the phase congruency value.

3.3.8 Processing Time

It represents the time required for the fusion process in seconds according to the computer specifications.

4 Experimental Results and Discussions

The implementations are based on five set of source images and the proposed hybrid technique (CVT-PCNN) is compared with existing techniques i.e. PCA, DWT, DCHWT, CVT and PCNN. The implementation is executed in MATLAB R2013b on windows 7 laptop with Intel Core I5 Processor, 4.0 GB RAM and 500 GB Hard Disk. The processed multimodality therapeutic input images are gathered from harvard medical school and radiopedia.org medical image online database. The size of the image is 512 × 512 for execution process.

4.1 Dataset 1

The MRI and PET are the input source images as shown in Figure-6A, B respectively. Figure-6I is the fused final output image of the proposed technique. The Existing techniques are PCA, DWT, DCHWT, CVT, Guided Filtering and PCNN outputs as shown in Figure-6C to H respectively.

4.2 Dataset 2

The MRI and PET are the input source images as shown in Figure-7A, B respectively. Figure 7I is the fused final output image of the proposed technique. The Existing techniques are PCA, DWT, DCHWT, CVT, Guided Filtering and PCNN outputs as shown in Figure-7C to H respectively.

4.3 Dataset 3

The MRI and PET are the input source images as shown in Figure-8A, B respectively. Figure 8I is the fused final output image of the proposed technique. The Existing techniques are PCA, DWT, DCHWT, CVT, Guided Filtering and PCNN outputs as shown in Figure-8C to H respectively.

4.4 Dataset 4

The MRI and SPECT are the input source images as shown in Figure-9A, B respectively. Figure 9I is the fused final output image of the proposed technique. The Existing techniques are PCA, DWT, DCHWT, CVT, Guided Filtering and PCNN outputs as shown in Figure-9C to H respectively.

4.5 Dataset 5

The MRI and PET are the input source images as shown in Figure-10A, B respectively. Figure 10I is the fused final output image of the proposed technique. The Existing techniques are PCA, DWT, DCHWT, CVT, Guided Filtering and PCNN outputs as shown in Figure-10C to H respectively.

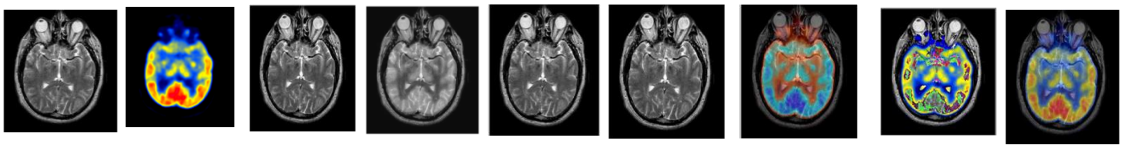

(A) MRI (B) PET (C) PCA (D)DWT (E) DCHWT (F)CVT (G)Guided Filtering (H) PCNN (I) Proposed Method

Figure 6: Results of Dataset 1

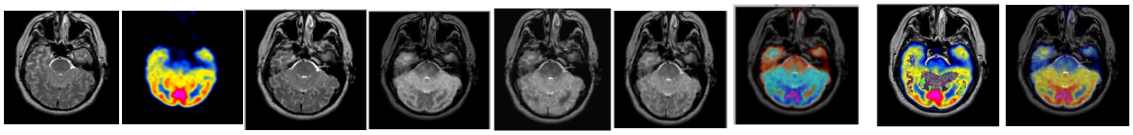

(A) MRI (B) PET (C) PCA (D)DWT (E) DCHWT (F)CVT (G)Guided Filtering (H) PCNN (I) Proposed Method

Figure 7: Results of Dataset 2

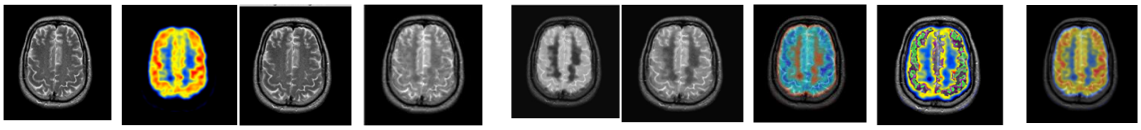

(A) MRI (B) PET (C) PCA (D)DWT (E) DCHWT (F)CVT (G)Guided Filtering (H) PCNN (I) Proposed Method

Figure 8: Results of Dataset 3

(A) MRI (B) SPECT (C) PCA (D)DWT (E) DCHWT (F)CVT (G)Guided Filtering (H) PCNN (I) Proposed Method

Figure 9: Results of Dataset 4

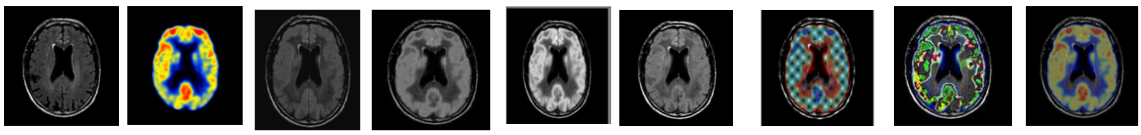

(A) MRI (B) PET (C) PCA (D)DWT (E) DCHWT (F)CVT (G)Guided Filtering (H) PCNN (I) Proposed Method

Figure 10: Results of Dataset 5

Table1. Performance Metrics obtained for different medical image fusion algorithms

Method	Metrics	PCA	DWT	DCHWT	CVT	GIF	PCNN	Proposed Method
Dataset 1	AG	0.0595	0.0743	0.07671	0.0741	0.0781	0.0861	**0.0924**
	STD	0.687	0.675	0.717	0.7284	0.886	0.868	**0.962**
	C_{local}	0.624	0.567	0.797	0.8125	0.856	0.882	**1.131**
	SSIM	0.798	0.836	0.872	0.7818	0.8921	0.7892	**0.9912**
	$Q^{AB/F}$	0.8384	0.8295	0.8618	0.8515	0.8382	0.8563	**0.9639**
	MI	0.8267	0.8392	0.8481	0.8614	0.8522	0.8714	**0.9852**
	FSIM	0.9451	0.9621	0.9619	0.9436	0.9573	0.9782	**0.9975**
	PT	2.286 sec	2.726 sec	2.862 sec	2.381 sec	2.582 sec	2.253 sec	**1.794 sec**
Dataset 2	AG	0.0893	0.0627	0.0692	0.0795	0.0828	0.0848	**0.0982**
	STD	0.5745	0.5791	0.6182	0.6785	0.6972	0.7023	**0.7742**
	C_{local}	0.6936	0.6691	0.7172	0.6818	0.7283	0.7431	**0.8729**
	SSIM	0.6578	0.6932	0.7021	0.6186	0.6283	0.6086	**0.7939**
	$Q^{AB/F}$	0.5468	0.5925	0.5639	0.5498	0.4698	0.5386	**0.6342**
	MI	1.0671	1.0482	1.3724	1.3815	1.5212	1.1733	**1.5813**
	FSIM	0.8756	0.8791	0.8723	0.8681	0.8526	0.8731	**0.9154**
	PT	2.462 sec	2.276 sec	2.381 sec	2.482 sec	2.832 sec	2.597sec	**2.098 sec**
Dataset 3	AG	0.0853	0.0779	0.0758	0.0846	0.0841	0.0813	**0.0953**
	STD	0.8534	0.935	0.963	0.987	0.927	0.938	**1.067**
	C_{local}	0.7652	0.682	0.637	0.752	0.619	0.741	**0.861**
	SSIM	0.6439	0.7382	0.7371	0.6783	0.6852	0.7726	**0.8521**
	$Q^{AB/F}$	0.6225	0.6718	0.6471	0.6921	0.6724	0.6619	**0.7652**
	MI	1.2583	1.1691	1.0162	1.5821	1.3216	1.5271	**1.7312**
	FSIM	0.9821	0.9242	0.9463	0.9216	0.9562	0.9673	**0.9845**
	PT	2.164 sec	2.472 sec	3.372 sec	3.182 sec	3.582 sec	2.672 sec	**2.012 sec**
Dataset 4	AG	0.6879	0.0638	0.0751	0.06917	0.0785	0.0812	**0.0997**
	STD	0.7295	0.782	0.724	0.691	0.748	0.785	**0.846**
	C_{local}	0.7324	0.665	0.678	0.6843	0.763	0.765	**0.8521**
	SSIM	0.9128	0.953	0.9361	0.9627	0.9732	0.9883	**1.097**
	$Q^{AB/F}$	0.6154	0.5374	0.5629	0.5672	0.5821	0.5374	**0.5953**
	MI	1.002	1.072	1.192	1.269	1.372	1.372	**1.6657**
	FSIM	0.7934	0.8482	0.9042	0.9174	0.9482	0.9572	**0.9873**
	PT	2.874 sec	3.638 sec	2.493 sec	3.103sec	3.391 sec	2.532 sec	**2.192 sec**
Dataset 5	AG	0.7542	0.0638	0.0751	0.0778	0.0785	0.0842	**0.0984**
	STD	0.7145	0.782	0.724	0.697	0.798	0.793	**0.8721**
	C_{local}	0.6256	0.665	0.678	0.646	0.764	0.773	**0.8512**
	SSIM	0.9164	0.965	0.993	0.9316	0.975	0.968	**1.1340**
	$Q^{AB/F}$	0.6148	0.5319	0.5629	0.5721	0.5723	0.5612	**0.5812**
	MI	0.9489	1.034	1.178	0.9987	1.381	1.8816	**1.5712**
	FSIM	0.7892	0.8818	0.9178	0.8762	0.9381	0.9481	**0.9812**
	PT	3.765 sec	3.869 sec	2.393 sec	2.579 sec	3.263 sec	2.572 sec	**2.101 sec**

Table 1 demonstrates the performance metrics experimental results of the traditional fusion algorithms and hybrid fusion algorithms on the dataset 1, 2, 3, 4 and 5. To evaluate the performance of the proposed image fusion approach MRI, PET and SPECT image are selected as the input source multimodal medical images. It can be seen that because of different imaging standards, the source images with various modalities contain integral data. The performance metrics are compared with the traditional methods like PCA, Discrete Wavelet Transform (DWT), Discrete Cosine Harmonic Wavelet Transform (DCHWT), Curvelet Transform, Guided Image Filtering (GIF) and Pulse Coupled Neural Network (PCNN) to the hybrid method (Curvelet Transform-PCNN). The evaluations of performance metrics for hybrid techniques results are better than other existing traditional techniques as shown in Table 1. By means of objective criteria analysis, the proposed algorithm not only preserves edge information but also improves the spatial detail information. Therefore, the proposed method of multimodal medical image fusion is an effective method in both subjective and objective evaluation criterion. The experimental results are shown in Figure 6, 7, 8, 9 and 10 and Table 1.

(A)

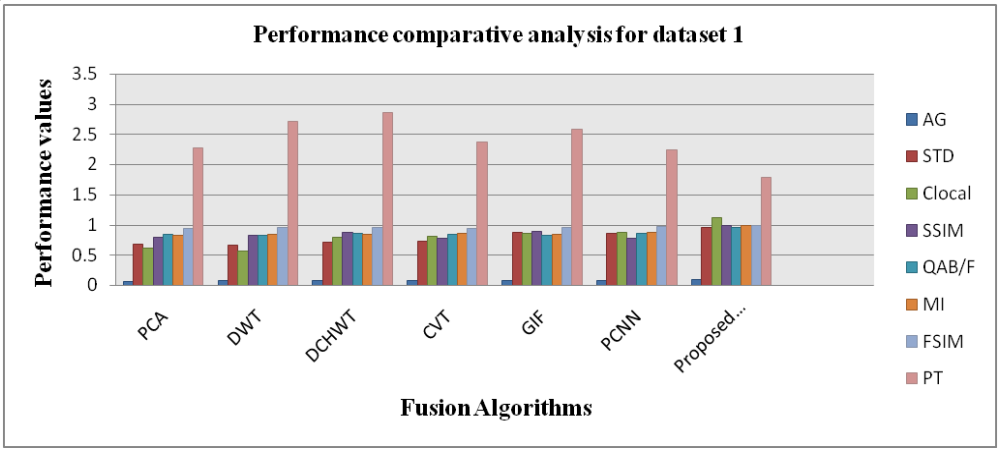

(B)

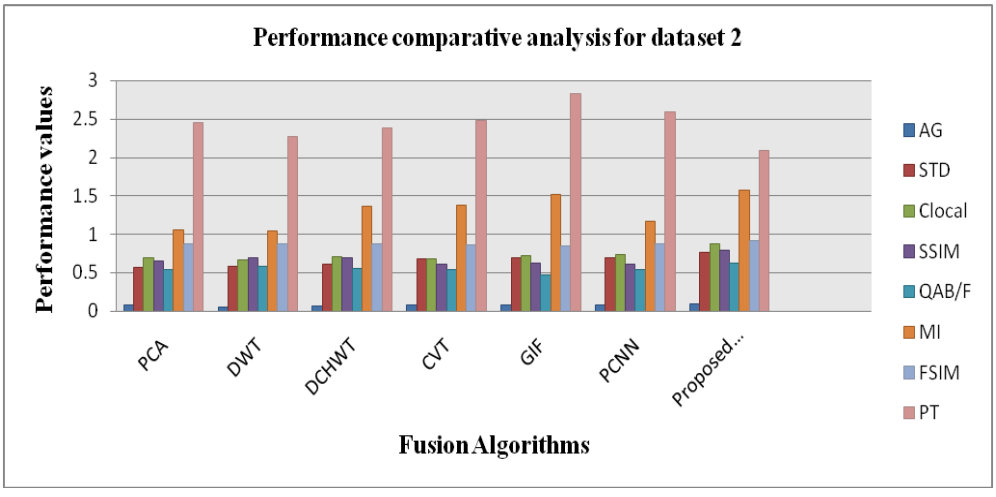

(C)

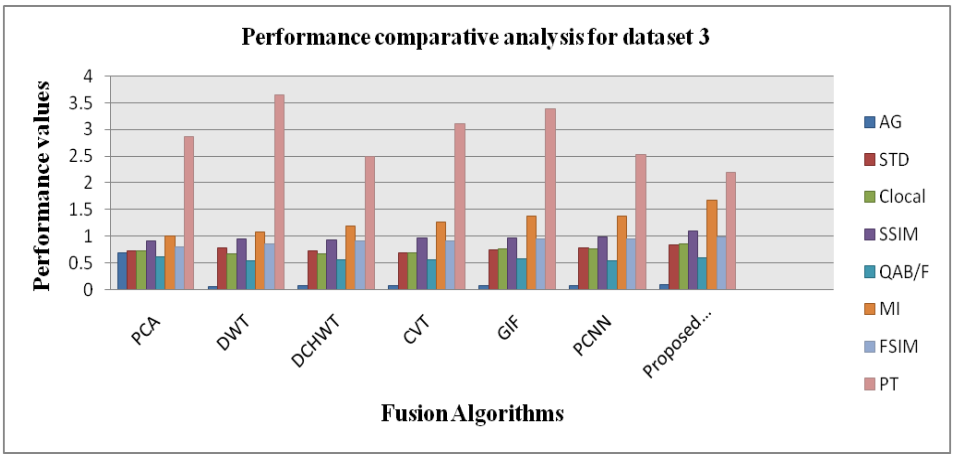

(D)

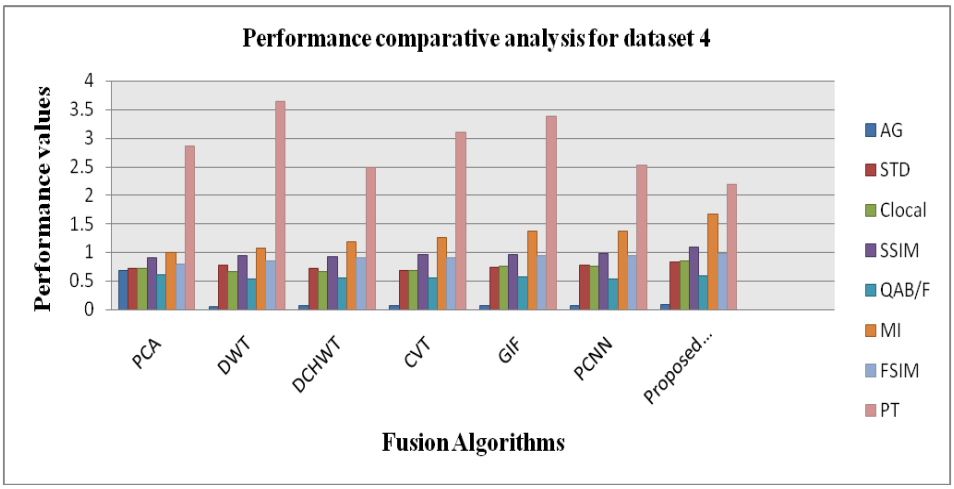

(E)

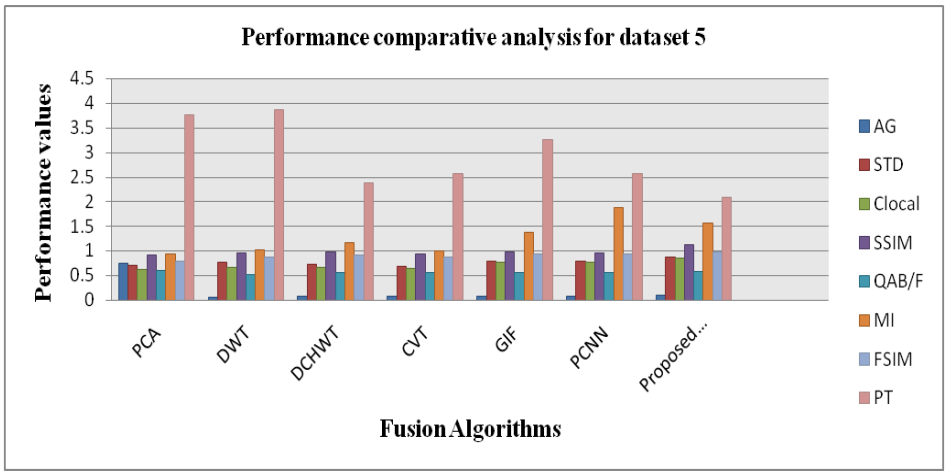

Figure.11 Performance Comparative analysis for 5 datasets (A-E)

The evaluated performance metrics output results are shown in Table 1. The superior performance value in each column of Table 1 is shown in bold. The graphs for all the values of Table 1 are shown in the Figure-11 A, B, C, D and E. From the Table 1 and Figure-11, it is clear the proposed hybrid technique outperform the existing techniques for all the performance metrics.

Conclusion

This work investigated the performance of both the traditional and hybrid multimodal medical image fusion techniques using several evaluation metrics. It has been shown that the best multimodality medical image fusion technique is implemented using proposed hybrid technique. This hybrid algorithm (Curvelet Transform-Pulse Coupled Neural Network) introduced a superior performance compared to all the other traditional techniques. It gives much more image details, higher image quality, the shortest processing time and a better visual inspection. All these advantages make it a good choice for several applications such as for assisting medical diagnosis for an accurate treatment.

References

[1] Jiao Du, Weisheng Li, Ke Lu, Bin Xiao "An Overview of Multi-Modal Medical Image Fusion" Elsevier, Neurocomputing-2015.
[2] Jiao Du,WeishengLi n,BinXiao,QamarNawaz "Union Laplacian pyramid with multiple features for medical image fusion" Elsevier, Neuro computing 194, 326–339-2016.
[3] xingbin Liu, Wenbo Mei, Huiqian Du "Structure tensor and nonsubsampled sheasrlet transform based algorithm for CT and MRI image fusion" Elsevier,Neurocomputing-2017.
[4] K.N. Narasimha Murthy and J. Kusuma "Fusion of Medical Image Using STSVD" Springer, Proceedings of the 5th International Conference on Frontiers in Intelligent Computing: Theory and Applications, Advances in Intelligent Systems and Computing 516-2017.
[5] Satishkumar S. Chavana, Abhishek Mahajanb, Sanjay N. Talbarc, Subhash Desaib, Meenakshi Thakurb, Anil D'cruzb "Nonsubsampled rotated complex wavelet transform (NSRCxWT) for medical image fusion related to clinical aspects in neurocysticercosis" Elsevier, Computers in Biology and Medicine 81,64–78-2017.
[6] S. Chavan, A. Pawar and S. Talbar "Multimodality Medical Image Fusion using Rotated Wavelet Transform" Advances in Intelligent Systems Research. Vol. 137, Pp. 627-635-2017
[7[Heba M. El-Hoseny, El-Sayed M. El.Rabaie, Wael Abd Elrahman, and Fathi E Abd El-Samie "Medical Image Fusion Techniques Based on Combined Discrete Transform Domains" 34th National Radio Science Conference (NRSC 2017), IEEE ,978-1-5090-4609-6/17-2017
[8] Udhaya Suriya TS , Rangarajan P, "Brain tumour detection using discrete wavelet transform based medical image fusion" Biomedical Research-2017
[9] Periyavattam Shanmugam Gomathi, Bhuvanesh Kalaavathi "Multimodal Medical Image Fusion in Non-Subsampled Contourlet Transform Domain" Scientific Research Publishing, Circuits and Systems, 7, 1598-1610-2016
[10] C.Karthikeyan and B. Ramadoss "Comparative Analysis of Similarity Measure Performance for Multimodality Image Fusion using DTCWT and SOFM with Various Medical Image Fusion Techniques" Indian Journal of Science and Technology, Vol 9(22), June 2016.

[11] Xinzheng Xua, Dong Shana, Guanying Wanga, Xiangying "Multimodal medical image fusion using PCNN optimized by the QPSO algorithm" Elsevier, Applied Soft Computing , 2016.
[12] Jyoti Agarwal and Sarabjeet Singh Bedi "Implementation of hybrid image fusion technique for feature enhancement in medical diagnosis" springer, Human-centric Computing and Information Sciences, 2015.
[13] Jing-jing Zonga, Tian-shuang Qiua, "Medical image fusion based on sparse representation of classified image patches" Elsevier, Biomedical Signal Processing and Control 34,195–205, 2017.
[14] Richa Gautam and Shilpa Datar "Application of image fusion techniques on medical images" International Journal of Current Engineering and Technology, 2017.
[15] Xiaojun Xu, Youren Wang, Shuai Chen "Medical image fusion using discrete fractional wavelet transform" Elsevier, Biomedical Signal Processing and Control 27, 103–111-2016
[16] Zhaobin Wang, Shuai Wang,Ying Zhu, Yide Ma "Review of image fusion based on pulse-coupled neural network" Springer, Arch Computer Methods Eng, 2015.
[17] Shutao Li, Xudong Kang S And Jianwen Hu "Image fusion with guided filtering" Transactions on Image Processing, Vol. 22, No. 7, July 2013.
[18] B. K. Shreyamsha Kumar "Multifocus and multispectral image fusion based on pixel significance using discrete cosine harmonic wavelet transform" Springer-Verlag London Limited, 2012.
[19] K. He, J. Sun, and X. Tang, "Guided image filtering," in Proc. Eur. Conf. Comput. Vis., Heraklion, Greece, pp. 1–14, Sep. 2010.
[20] Z. Farbman, R. Fattal, D. Lischinski, and R. Szeliski, "Edge-preserving decompositions for multi-scale tone and detail manipulation," ACM Trans. Graph., vol. 27, no. 3, pp. 67-1–67-10, Aug. 2008.
[21] F. Durand and J. Dorsey, "Fast bilateral filtering for the display of highdynamic-range images" ACM Trans. Graph., vol. 21, no. 3, pp. 257–266,Jul. 2002.
[22] N. Draper and H. Smith, Applied Regression Analysis. New York, USA:Wiley, 1981.
[23] Narasimhan, S.V., Harish, M.: Discrete cosine harmonic wavelet transform and its application to subband spectral estimation using modified group delay. In: Pai, B.R. Dr. (eds.) Proceedings of Conference in Honor of Dr.B.R. Pai.NationalAerospace Laboratories, Bangalore, 2004.
[24] Narasimhan, S.V, Harish, M., Haripriya, A.R., Basumallick, N.: Discrete cosine harmonic wavelet transform and its application to signal compression and subband spectral estimation using modified group delay. J. SIViP 3(1), 85–99, 2009.
[25] Narasimhan, S.V., Haripriya, A.R., Shreyamsha Kumar,B.K.: Improved Wigner–Ville distribution performance based on DCT/DFT harmonic wavelet transform and modified magnitude group delay. Signal Process. 88(1), 1–18, 2008.
[26] Narasimhan, S.V., Veena, S.: Signal Processing: Principles and Implementation, Revised Edition. Narosa Publishing House Pvt. Ltd, India, 2008.
[27] Britanak, V., Yip, P.C., Rao, K.R.: Discrete Cosine and Sine Transforms.1st edn. Academic Press, Great Britain, 2007.
[28] RAJESH, M. "A SYSTEMATIC REVIEW OF CLOUD SECURITY CHALLENGES IN HIGHER EDUCATION." The Online Journal of Distance Education and e- Learning 5.4 (2017): 1.
[29] Rajesh, M., and J. M. Gnanasekar. "Protected Routing in Wireless Sensor Networks: A study on Aimed at Circulation." Computer Engineering and Intelligent Systems 6.8: 24-26.

[30] Rajesh, M., and J. M. Gnanasekar. "Congestion control in heterogeneous WANET using FRCC." Journal of Chemical and Pharmaceutical Sciences ISSN 974 (2015): 2115.
[31] Rajesh, M., and J. M. Gnanasekar. "Hop-by-hop Channel-Alert Routing to Congestion Control in Wireless Sensor Networks." Control Theory and Informatics 5.4 (2015): 1-11.
[32] Rajesh, M., and J. M. Gnanasekar. "Multiple-Client Information Administration via Forceful Database Prototype Design (FDPD)." IJRESTS 1.1 (2015): 1-6.
[33] Rajesh, M. "Control Plan transmit to Congestion Control for AdHoc Networks." Universal Journal of Management & Information Technology (UJMIT) 1 (2016): 8-11.
[34] Rajesh, M., and J. M. Gnanasekar. "Consistently neighbor detection for MANET." Communication and Electronics Systems (ICCES), International Conference on. IEEE, 2016.
[35] https://radiopaedia.org.
[36] http://www.med.harvard.edu.